GEOLOGICA CARPATHICA, 2026, 77, 3, 237–253 https://doi.org/10.31577/GeolCarp.2026.12

Tanyeri–Yedisu seismic gap along the Erzincan–Varto section of the North Anatolian Fault: Age, displacement, slip rate and return period in Eastern Türkiye

ALI KOÇYIĞIT[1], ŞULE GÜRBOĞA[2,✉] and AYDIN ÇIÇEK[3]

[1]Middle East Technical University, Department of Geological Engineering, Active Tectonics and Earthquake Research Lab., Ankara, Türkiye
[2]İstanbul Technical University, Faculty of Mines, Department of Geological Engineering, İstanbul, Türkiye
[3]General Directorate of Mineral Research and Exploration, Ankara, Türkiye

(Manuscript received October 1, 2025; accepted in revised form May 19, 2026; Associate Editor: Giovanni Barreca)

Abstract: The study area is situated in the easternmost segment of the North Anatolian Fault System (NAFS), including the Karlıova triple junction (KTJ) where the NAFS intersects the East Anatolian Fault System (EAFS). The regional angular unconformity between intensely deformed pre-Quaternary rocks and the overlying undeformed neotectonic deposits clearly indicates that the onset of the strike-slip neotectonic regime and the formation of the related structures, namely the NAFS and EAFS, occurred in the early Quaternary (2.588 Myr). The present study focuses on the long-term (241-year) Tanyeri–Yedisu seismic gap, the onset age of the strike-slip neotectonic regime, and several key parameters of the Erzincan–Varto section of the NAFS. These are total dextral displacement, average slip rate, and the return period of the peak earthquake expected from the Tanyeri–Yedisu seismic gap. New field data, obtained from the detailed field geological mapping of the region, using the displacement of the Inner Tauride Suture as a structural marker and the Yedisu River as a geographic marker, clearly show that the total dextral displacement is 57 km. This offset was accumulated over an approximately a 2.6 Myr time interval. These values correspond to an average slip rate of 22 mm/yr and a return period of 205±50 years for the peak earthquake originating from the Tanyeri–Yedisu seismic gap.

Keywords: neotectonic regime, fault system, seismic gap, total displacement, slip rate, return period

Introduction

The Erzincan–Varto section of the North Anatolian Fault System (NAFS) is a key locality for strike-slip neotectonic domains. It is located within the East Anatolian Tectonic Block (EATB), bounded by the Kelkit–Çoruh fault zones to the northwest, the NAFS and Bitlis–Zagros Suture Zone (BZSZ) to the southwest, the Lesser Caucasus to the northeast, and the Turkish–Iranian border to the east (Fig. 1b). The area is defined by a strike-slip neotectonic regime (Koçyiğit & Canoğlu 2017), combining simultaneous extension and contraction. Within the EATB, the fault pattern includes NE- and NW-trending sinistral and dextral faults, N–S oblique-slip normal faults, E–W thrust and reverse faults, and intervening pull-apart basins (Fig. 1b). GPS data and recent seismic activity confirm that all of these structures are seismically active (Koçyiğit 1983, 2013, 2023; Reilinger et al. 1997, 2006; ERD 2000, 2020, 2023; Tan et al. 2008). This is evidenced by the occurrence of destructive earthquakes originating from the NE-trending sinistral, NW-trending dextral and approximately E–W-trending reverse faults (Fig. 1b and Table 1). In addition, the Nemrut strato-volcano was also reactivated during the 1441 historical earthquake, with basaltic lavas erupting from an N–S-trending open fracture (fissure) that cut across the summit of the volcanic cone.

The Tanyeri–Yedisu area is located within the Koçyatağı (Erzincan)–Yedisu, Elmalı–Kaynarpınar, and Kızılçubuk–Ilıpınar–Varto (Muş) sections of the NAFS (rectangular inserts in Figs. 1, 2). The evolution of both the strike-slip neotectonic regime and its associated structures is well recorded in the coeval deposits of the basin. Five major strike-slip basins occur in the Erzincan–Karlıova section of the NAFS, namely, from west to east, the Erzincan, Yedisu, Başköy, Kaşıkçı and Karlıova pull-apart basins (Fig. 2). The dextral strike-slip faults are particularly prominent in this section. They are active and have the potential to generate devastating earthquakes $M_w \geq 7.0$. This is further evidenced by the occurrence the 26 December 1939, M_w 7.9 Erzincan earthquake (1 in Fig. 1b and 2 in Fig. 2).

The earthquake originated from the Karadağ master fault segment and then propagated west-northwestward for a distance of 360 km along the NAFS (Koçyiğit & Tokay 1985; Koçyiğit 1989, 1990). The largest coseismic dextral offset, measured very close to the epicenter, was 9.4 m (Fig. 3). This is the largest strike-slip earthquake to date in Türkiye. In addition, following the Erzincan earthquake, several moderate-sized M_w [5.6, 6.8] destructive earthquakes, some producing surface ruptures, occurred in the Erzincan–Karlıova area (Fig. 2 and Table 2). One of these was the 13 March 1992, Ms 6.8 Saztepe (Erzincan) earthquake. The last major historical

✉ corresponding author: Şule Gürboğa
sulegurboga@gmail.com

CC BY NC ND

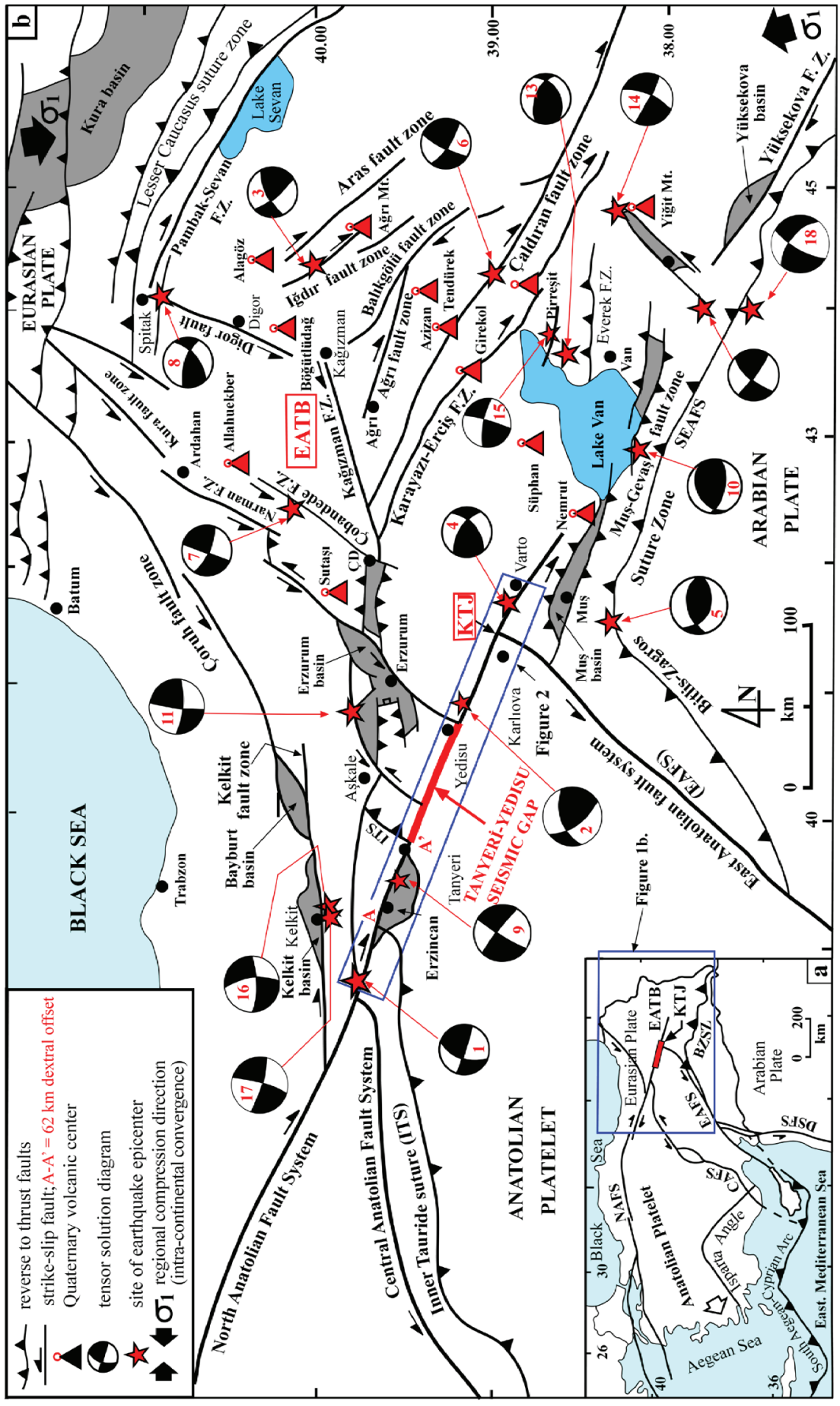

Fig. 1. (a) Simplified map illustrating plate tectonic configuration of Türkiye and the study area (rectangular insert in red color). BZSZ – Bitlis–Zagros suture zone, CAFS – Central Anatolian Fault System, DSFS – Dead Sea Fault System, EAFS – East Anatolian Fault System, KTJ – Karlıova Triple Junction, NAFS – North Anatolian Fault System; **(b)** Simplified seismotectonic map of Eastern Anatolia, and the Tanyeri–Yedisu seismic gap area (rectangular insert). EATB – East Anatolian Tectonic Block (Koçyiğit 2013, 2023; ERD 2000, 2020, 2023; Tan et al. 2008).

Table 1: Significant earthquakes took place in East Anatolian Tectonic Block (EATB) and its near environ in the period of 1939–2023.

No	Date	Time	Coordinates	Focal Depth	Magnitude	Geographic location	Risk	Source of earthquake	References
18	2023.12.31	17:06	37.53°N, 43.99°E	3 km	M_w=4.5	Yüksekova	Walls of 28 houses were cracked	Sinistral strike-slip fault	ERD (AFAD) 2023
17	2023.12.18	20:23	39.92°N, 39.29°E	7 km	M_w=4.1	Yeşilyurt–Kelkit		Sinistral strike-slip fault	ERD (AFAD) 2023
16	2023.12.17	22:15	39.93°N, 39.32°E	15 km	M_w=4.3	Yeşilyurt–Kelkit		Sinistral strike-slip fault	ERD (AFAD) 2023
15	2022.06.12	18:35	38.80°N, 47.70°E	10 km	M_w=5.1	Akçift (Muradiye)		Dextral strike-slip fault	KOERI (2020)
14	2020.02.23	16:00	38.40°N, 44.80°E	16 km	M_w=6.0	Kaşkol (Başkale)	9 deaths, 37 injured, over 100 structures were collapsed	Sinistral strike-slip fault	ERD (2020)
13	2011.10.23	12:41	38.90°N, 43.60°E	16 km	M_w=7.2	Tabanlı (Van)	644 deaths, 28,532 structures were damaged	Reverse fault	Irmak et al. (2012) KOERI (2011)
12	2005.01.25	18:44	37.71°N, 43.77°E	13.7 km	M_w=5.9	Sütlüce (Hakkari)	Two deaths, over 200 structures were collapsed	Sinistral strike-slip fault	HARVARD (2004)
11	2004.03.25	21:30	39.77°N, 40.88°E	10 km	M_w=5.6	Aşkale (Erzurum)	9 deaths, over 300 structures were ruined	Sinistral strike-slip fault	Tan et al. (2008)
10	2000.11.15	15:05	38.41°N, 42.95°E	48 km	M_w=5.7	Altınsaç (Gevaş)		Reverse fault	ERD (2000)
9	1992.03.13	17:18	39.71°N, 39.60°E	23 km	M_w=6.3	Saztepe (Erzincan)	653 deaths, 6702 structructure were collapsed	Dextral strike-slip fault	Tan et al. (2008)
8	1988.12.07	07:41	40.94°N, 44.29°E	10 km	M_w=6.7	Spitak (Armenia)	25,000 deaths, 90 % of Spitak was destroyed	Reverse fault with strike-slip component	Ambraseys (2001)
7	1983.10.30	04:12	40°.28N, 42°.18E	15 km	M_w=6.7	Çobandede–Horasan	1330 deaths, 2341 structures were ruined	Sinistral strike-slip fault with reverse component	Ambraseys (2001) Toksöz et al. (1983)
6	1976.11.24	12:22	39.10°E, 44.00°E	10 km	M_w=7.2	Çaldıran (Van)	3840 deaths, 9232 structures were collapsed	Dextral strike-slip fault	Ambraseys (2001) Toksöz et al. (1977)
5	1975.09.06	09:20	38.55°N, 40.75°E	5 km	M_w=6.5	Lice (Diyarbakır)	2384 deaths, 8149 structures were ruined	Reverse fault with strike-slip component	Ambraseys (2001)
4	1966.08.19	12:22	39.20°N, 41.40°E	16 km	M_w=6.8	Varto	2529 deaths, 34,000 structures were ruined	Reverse fault with strike-slip component	Ambraseys (2001) Eyidoğan (1992) Eyidoğan et al. (1991)
3	1962.09.04	22:59	40.00°N, 44.00°E	33 km	M_w=5.8	Iğdır	One death, over 100 structures were collapsed	Dextral strike-slip fault	Eyidoğan et al. (1991)
2	1949.08.17	18:44	39.40°N, 40.65°E	40 km	M_w=6.5	Elmalı (Karlıova)		Reverse fault	Kalafat et al. (2011) Tan et al. (2008)
1	1939.12.26	23:57	39.70°N, 39.70°E	35km	M_w=8.0	Koçyatağı – ERZ	40,000 deaths, 360 km long SR	Dextral strike-slip fault	Tan et al. (2008) Eyidoğan et al. (1991)

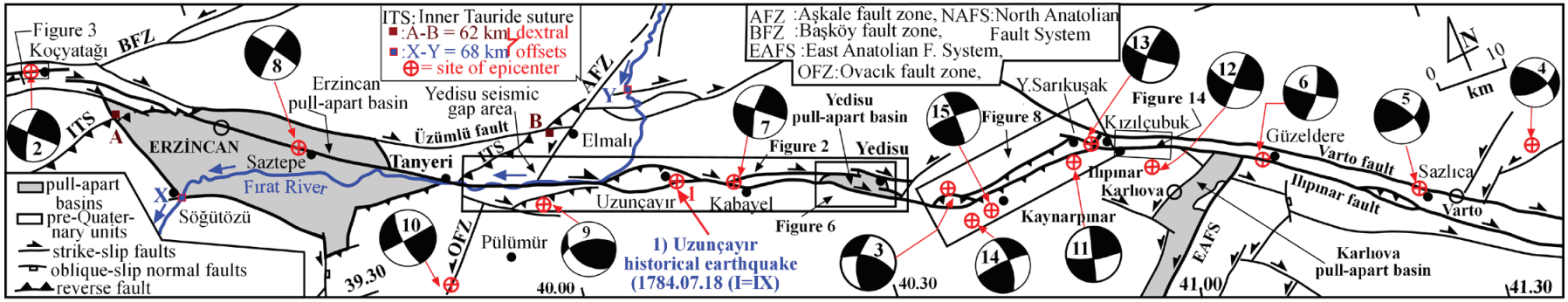

Fig. 2. Simplified seismotectonic map of the Koçyatağı (Erzincan)–Varto (Muş) section of the North Anatolian Fault System (NAFS) that illustrates the studied type localities (rectangular inserts). ITS – Inner Tauride Suture Zone (focal mechanism solutions from Tan et al. 2008 and ERD 2023).

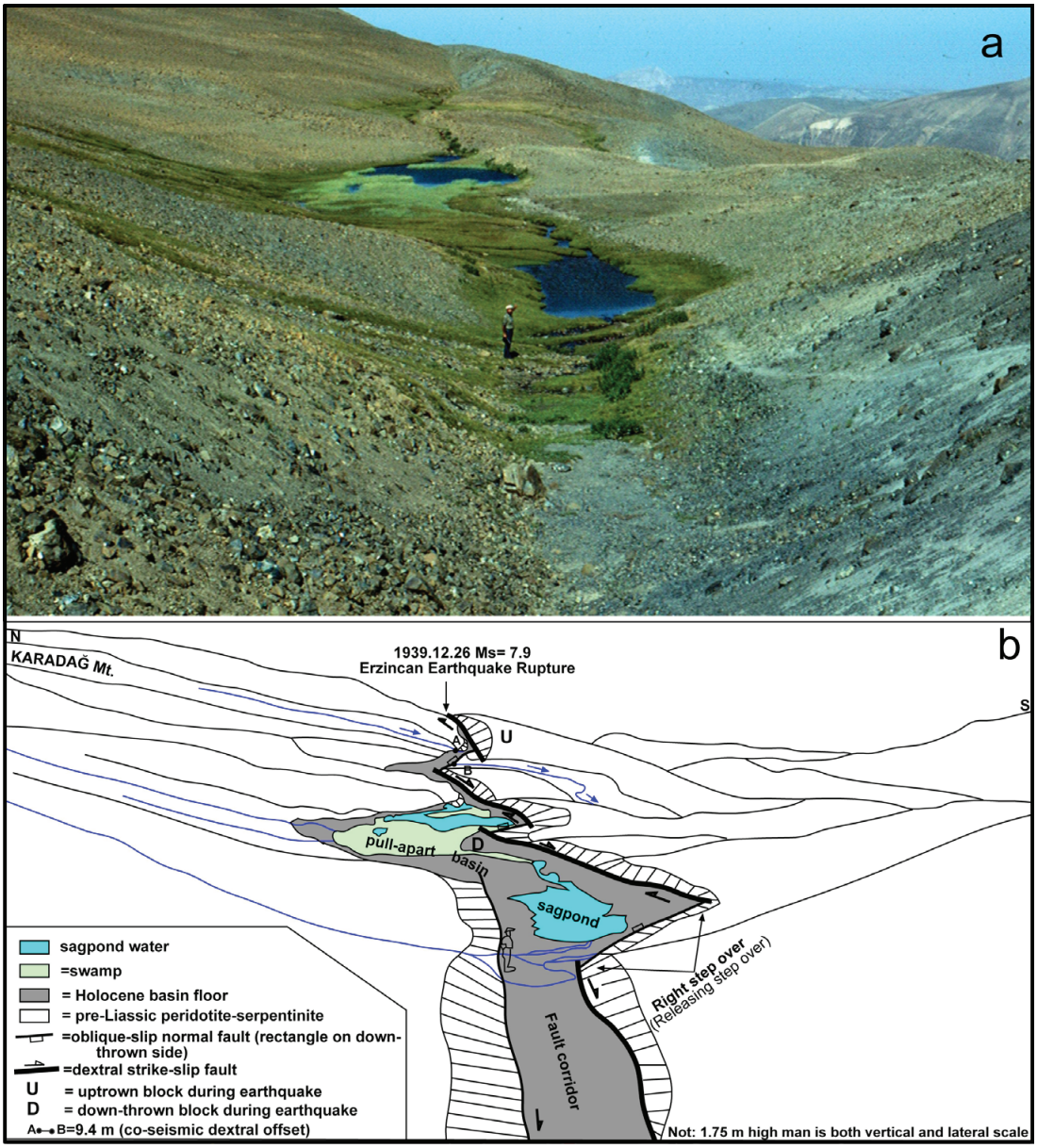

Fig. 3. (a) Field photograph of well-preserved strike-slip faulting-related features resulted from the largest 1939 Erzincan earthquake on the northeastern side of the Karadağ Mountain (view to W); **(b)** Redrawing and analysis of coseismic strike-slip faulting-induced co-seismic features.

earthquake on the Tanyeri–Yedisu section of the NAFS was the 1784 Uzunçayır earthquake (1 in Fig. 2). Since then, the accumulation of elastic strain energy has continued along the 73 km-long Tanyeri–Yedisu section. Based on both the slip rate and the length of the segments along the NAFS, the average return period of large earthquakes originating from the master fault segment of the NAFS is estimated to be about 230–280 years (Wells & Coppersmith 1994). When the average return periods of large earthquakes are taken into account, the Tanyeri–Yedisu section can be defined as a long-term seismic gap (Koçyiğit 2013). For instance, the average recurrence intervals of large earthquakes along the NAFS and EAFS are approximately 230–280 years and 500–750 years, respectively. The considerable difference between the two systems is clearly related to the slip rates, which are 22–24 mm/yr along the NAFS and about 11 mm/yr along the EAFS. Most recently, two moderate-sized earthquakes occurred in the Elmalı–Kaynarpınar area, located at the eastern end of the Yedisu seismic gap. These were the 14 June 2020, M_w 5.8 Bargi earthquake and the 15 June 2020, M_w 5.4 Kaynarpınar Plateau earthquake (Fig. 2, Table 2). Despite these seismic events have occurred, the Yedisu seismic gap has not yet been activated. The Erzincan–Karlıova section of the NAFS has been extensively studied through field geological mapping over the last thirty-four years.

Table 2: Some destructive earthquakes happened in the Erzincan–Varto section of the NAFS in 1784 and instrumental period of 1939–2022.

No	Date	Coordinates	Depth (km)	Magnitude	Geographic location	Type of fault	References
16	2022.09.16	39.40°N, 40.70°E	15	M_w=4.9	Cevizli stream (Yedisu)	Strike-slip	KOERI (2022)
15	2020.06.15	39.37°N, 40.74°E	7	M_w=5.6	Kaynarpınar plateau (Yedisu)	Strike-slip	ERD (2020)
14	2020.06.14	39.36°N, 40.71°E	8	M_w=5.8	Bargi (Yedisu)	Strike-slip	ERD (2020)
13	2005.06.06	39.30°N, 41.02°E	10	M_w=5.7	Kızılçubuk (Karlıova)	Strike-slip	USGS (2005)
12	2005.03.14	39.33°N, 40.91°E	24	M_w=5.9	Ilıpınar (Karlıova)	Strike-slip	Kalafat et al. (2011)
11	2005.03.12	39.39°N, 40.94°E	8	M_w=5.7	Kızılçubuk (Karlıova)	Strike-slip	Kalafat et al. (2011)
10	2003.01.27	39.48°N, 39.78°E	10	M_w=6.1	Pülümür	Strike-slip	Kalafat et al. (2011) Tan et al. (2008)
9	1992.03.15	39.53°N, 39.93°E	29	M_S=5.8	Yarbaşı (Pülümür)	Reverse	Kalafat et al. (2011)
8	1992.03.13	39.71°N, 39.60°E	23	M_S=6.8	Saztepe (Erzincan)	Strike-slip	Kalafat et al. (2011)
7	1967.07.26	39.50°N, 40.30°E	30	M_w=5.9	Kabayel (Erzincan)	Strike-slip	Kalafat et al. (2011)
6	1966.08.20	39.30°N, 41.16°E	33	M_w=5.7	Güzeldere (Karlıova)	Strike-slip	Kalafat et al. (2011)
5	1966.08.19	39.20°N, 41.40°E	26	M_S=6.8	Sazlıca (Varto)	Reverse	Kalafat et al. (2011)
4	1966.03.07	39.20°N, 41.60°E	26	M_w=5.6	Varto	Reverse	Tan et al. (2008) Kalafat et al. (2011)
3	1949.08.17	39.40°N, 40.65°E	40	M_w=6.5	Elmalı (Karlıova)	Reverse	Kalafat et al. (2011)
2	1939.12.26	39.90°N, 39.20°E	20	M_S=7.9	Koçyatağı (Erzincan)	Strike-slip	Kalafat et al. (2011)
1	1784.07.18	39.51°N, 40.20°E	?	I_o=IX	Uzunçayır (Yedisu)	Strike-slip	Ambraseys (1978) Ambraseys & Jackson (1998)

The main objective of this study is to introduce the Tanyeri–Yedisu seismic gap and to draw the attention to the potential seismic hazard that may occur in the future. The second goal is to contribute to the understanding of these geological problems; namely, the onset age of the neotectonic regime in eastern Türkiye, in light of both field geological and seismological data.

Stratigraphic outline

Two main rock assemblages are exposed along the Erzincan–Varto section of the NAFS. These are (1) the deformed paleotecc units, which are folded and affected by thrust and reverse faulting, and (2) nearly flat-lying, undeformed neotectonic units.

Paleotecc units consist of the Upper Cretaceous ophiolitic mélange; the Campanian–Maastrichtian deep-marine forearc sequence, which is coeval with the development of the ophiolitic mélange; the Lower–Middle Eocene marine to continental volcano-sedimentary sequence; the Oligocene–Lower Miocene shallow-marine to continental sedimentary sequence; and the Upper Miocene–Pliocene volcanics (basalt, andesite, and their pyroclastites) together with a fluvio-lacustrine sedimentary sequence. The neotectonic units, which rest with an angular unconformity on the paleotecc rocks, are represented by Quaternary fluvial deposits confined to the pull-apart basins. A detailed description and stratigraphy of the paleotecc units are beyond the scope of this study. Therefore, readers more information about these older units are referred to previous publications (Şaroğlu & Yılmaz 1986; Yılmaz et al. 1988; Koçyiğit 1990, 1991, 2013; Tutkun & Hancock 1990; Tarhan 1991; Ambraseys 2001; Koçyiğit et al. 2001). Stratigraphically, the present paper focuses mainly on the Yedisu basin and its immediate surroundings, where two paleotecc units are exposed. These are the ophiolitic mélange (combination of both the Inner Tauride ophiolitic complex and the Anatolian Nappe) and the deep-marine forearc sequence (Sütpınar Formation) (Figs. 4, 5).

Ophiolitic mélange (Anatolian Nappe)

The East Anatolian Plateau is largely underlain by two Upper Cretaceous ophiolitic mélange complexes of different origins (Dewey 1976): the northern Neo-Tethys mélange and the Inner Tauride Ocean mélange, mapped as the "Inner Tauride ophiolitic complex" and the "Anatolian Nappe" (Koçyiğit 1990, 1991). Exposed in separate outcrops along the Izmir–Ankara–Erzincan and Inner Tauride suture zones, these units were tectonically transported, strongly deformed, and stacked into a southward-overturned imbricate pile over 2 km thick during the prolonged intracontinental convergence between Arabia and Eurasia. The mélange commonly has faulted contacts with the Campanian–Pliocene cover units, although locally its top passes gradationally or erosively into them; the base is mostly unexposed. It is widely exposed along the northern margin of the Yedisu Basin, with smaller isolated occurrences inside the basin and grades northwards and west-southwestwards into a deep-marine forearc sequence (Figs. 4, 5). Lithologically, it is a tectono-sedimentary mixture of diverse, rootless blocks of various sizes, ages, and facies, enclosed in a matrix of intensely sheared sandstone, siltstone and black shale rich in ophiolitic debris. The blocks include ultramafic and mafic rocks (dunite, harzburgite, serpentinite, gabbro, diabase, and pillow basalt), volcaniclastic and sedimentary rocks (ignimbrite, graywacke, radiolarite, manganese nodules, and Cambrian–Ordovician shale to Jurassic–Cretaceous limestone and chert). They range from centimeter-scale clasts to mappable megablocks; some preserve bedded successions 30 m to 1 km thick. Litho- and biofacies indicate

derivation from ocean-floor, continental rise–slope, shelf, and forearc settings. The youngest fossil assemblage in the matrix is Santonian–early Campanian, and the mélange locally shows a gradational upper contact with the Campanian–Maastrichtian forearc succession (Koçyiğit 1990). Collectively, these data indicate that the ophiolitic mélange formed along an active continental margin before the Maastrichtian and was later tectonically transported to its present position, where it was thrust over the Campanian–Pliocene cover sequences (Koçyiğit 2013).

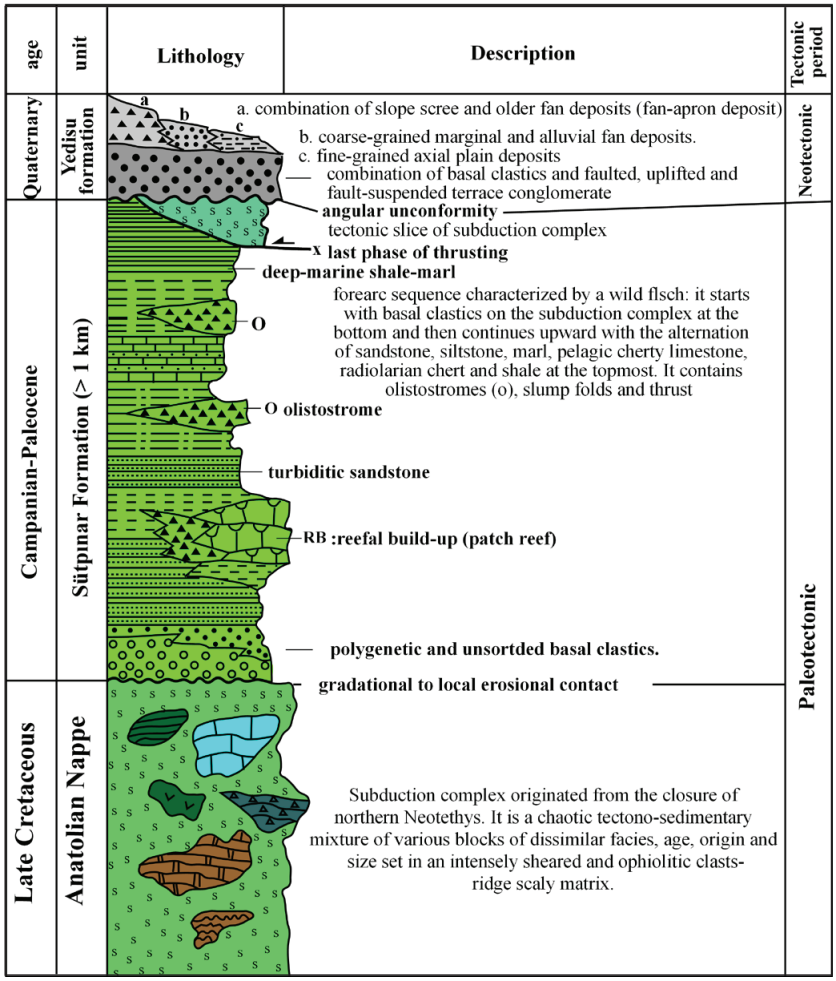

Fig. 4. Combined stratigraphical columnar section of the Yedisu and its near environment.

Sütpınar Formation

The Sütpınar Formation has its type locality near the village of Sütpınar, located west-southwest of the Erzincan pull-apart basin, outside the study area. It is widely exposed along the southern margin of the Yedisu pull-apart basin (Fig. 5) and, further north-northeast, conformably overlies the ophiolitic mélange. Within the basin, it is tectonically juxtaposed against the mélange and overlain by Quaternary basin fill deposits with an angular unconformity (Fig. 5). Outside the basin, the formation begins with mélange-derived basal clastics and transitions upward into turbiditic sandstone, laminated black shale-marl alternation, pelagic cherty limestone, reefal patches and conglomerate intercalations. The basal clastics are unsorted and polygenic, composed of mélange-derived pebbles and boulders embedded in a sandy matrix. Turbiditic sandstone beds, ranging from a few cm to 1.4 m in thickness, exhibit graded bedding and sole structures such as groove and flute casts. Lenticular olistostromes, slump folds, and slump thrusts are common, accompanied by rare mélange-derived olistoliths. These features indicate deposition in a tectonically unstable forearc environment during the Campanian–Maastrichtian (Koçyiğit 2013). The formation's apparent thickness exceeds 1 km.

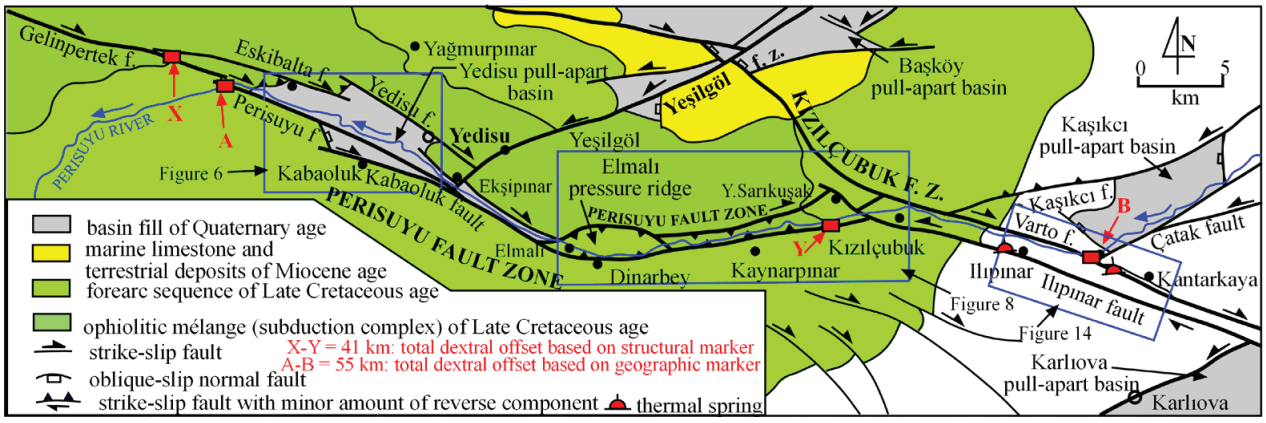

Fig. 5. Simplified geological map of the Yedisu basin and its near environment.

Neotectonic units (basin fill)

These units formed in a strike-slip neotectonic regime starting at the beginning of Quaternary and fill the Yedisu pull-apart basin (Fig. 4). The neotectonic units are almost flat-lying and undeformed, except along faults, where they are uplifted as pressure ridges or juxtaposed against older paleotectonic rocks. They overlie all pre-Quaternary paleotectonic units with an angular unconformity. The deposits are grouped into two facies: (1) marginal facies with basal conglomerates and older and recent fan-apron deposits, and (2) depocenter facies with fluvial, floodplain and marsh deposits.

Basal conglomerates and older fan-apron deposits are the most widespread neotectonic units and are extensively exposed as fault-terrace deposits along the faulted margins of the Yedisu pull-apart basin. They form pressure ridges and faulted, uplifted, dissected, fault-suspended terraces (Figs. 6, 7). Coarse-grained deposits are steeply tilted to overturned within fault-bounded pressure ridges and along fault contacts, but remain nearly flat-lying away from these structures. Older fan-apron deposits are gray, unsorted, weakly lithified to lose, massive, polygenic boulder conglomerates with coarse-grained sandstone lenses. They are dominated by mélange-derived clasts (peridotite, gabbro, serpentinite, radiolarite, chert, spilitic basalt, andesite, recrystallised and reefal limestone, and sandstone). These were eroded from paleotectonic units and deposited in alluvial fans by high-energy debris flows and fluvial systems such as the Perisuyu River (Fig. 7), then faulted, uplifted, dissected, and exposed as fault-suspended terraces. The conglomerates have a sandy, ophiolite-rich matrix, weakly cemented by calcite, and reach a total thickness of about 60 m.

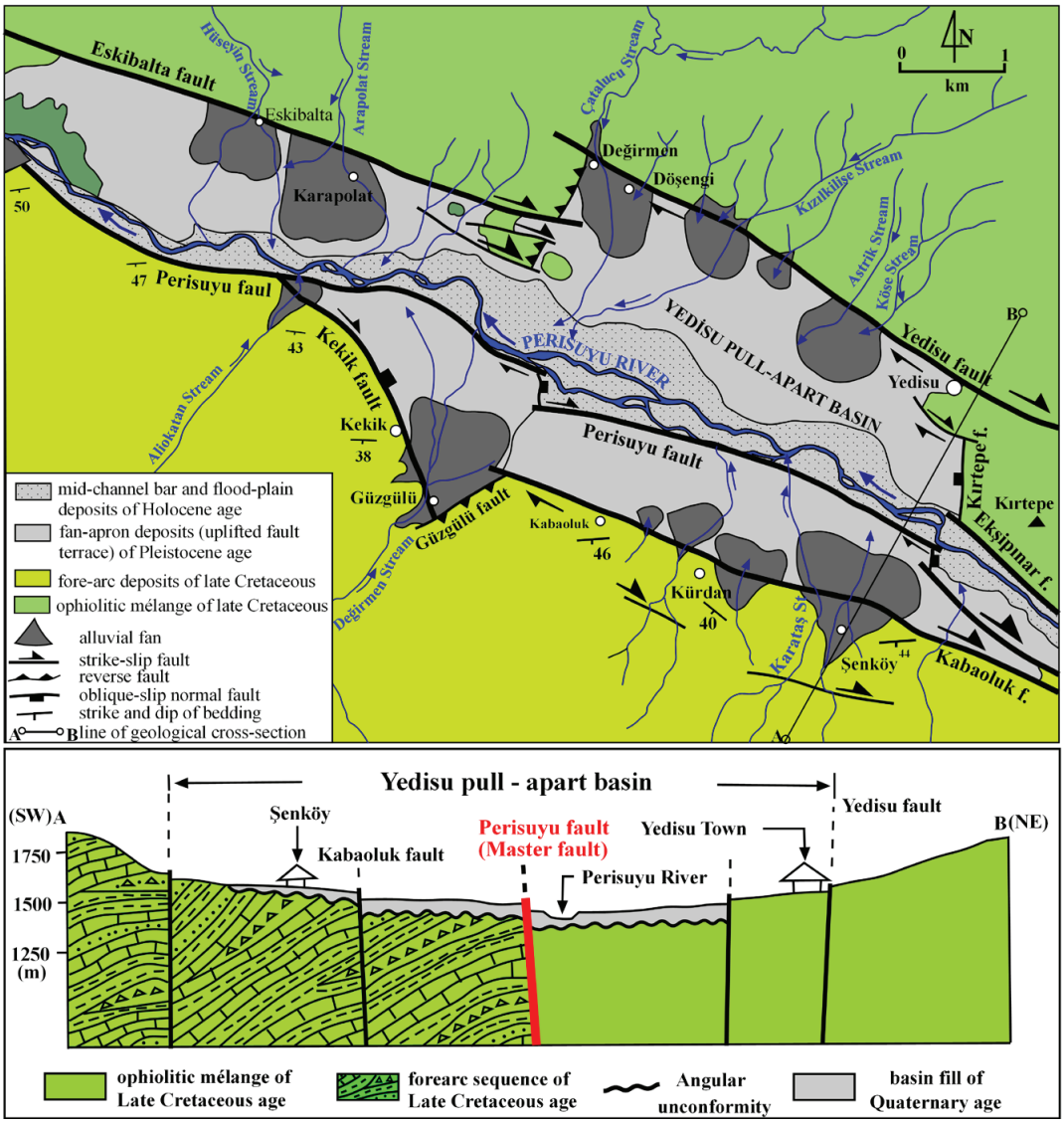

Fig. 6. (a) Geological map of the Yedisu pull-apart basin. **(b)** Geological cross-section along the Line A–B in Fig. 6a. It illustrates two-dimensional structure of the Yedisu pull-apart basin.

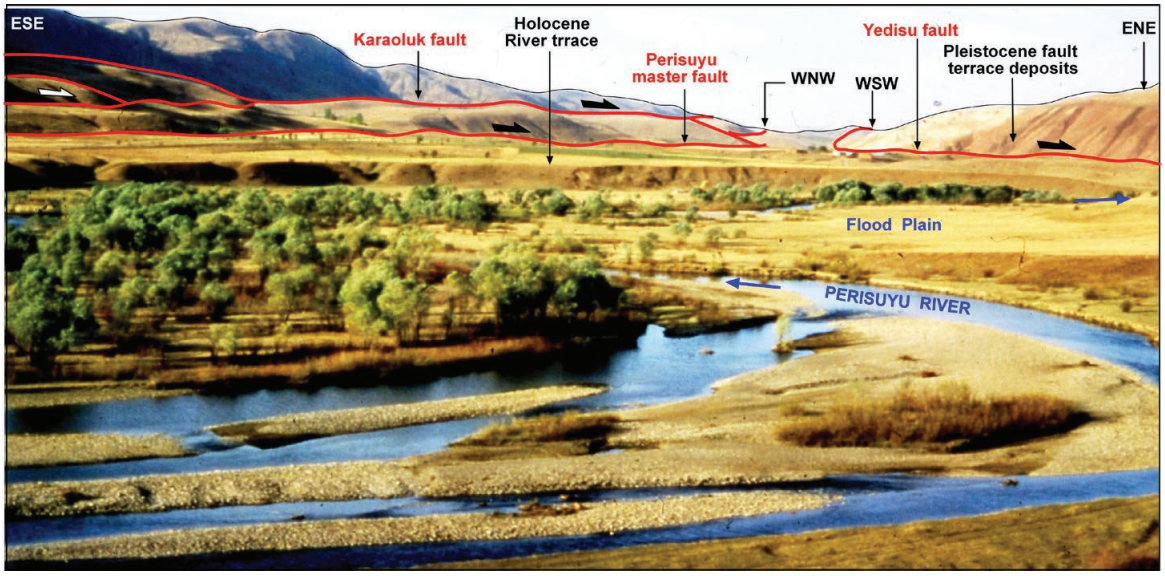

Fig. 7. Field photograph illustrating the central section of the Yedisu pull-apart basin drained by the Yedisu River (view to W).

Younger fan-apron deposits and recent alluvial fans are widely distributed along both the northern and southern fault-bounded margins of the Yedisu pull-apart basin (Fig. 6), forming a lens-shaped blanket of unconsolidated sediments about 0.5–1.4 km wide and 7–10 km long. They result from the coalescence of alluvial fans and talus deposits. These fans formed at the mouths of transverse streams draining the highest margin-bounding highlands towards the basin, where sediments of all sizes were eroded, transported and deposited along the steep, fault-controlled mountain front. Thus, the fans show a systematic fining from coarse-grained material at the apex to fine-grained deposits distally, and their clasts are generally sub-rounded to rounded. In contrast, the talus consists of unsorted, angular material transported and accumulated by gravity on slopes and at the base of fault scarps. Over time, these two sedimentary packages merged into a thick blanket, up to 100 m thick, that primarly covers the northern and southern margins of the basin (Fig. 6).

One side of this blanket is fault-bounded, whereas the opposite side passes vertically and laterally into finer-grained depocenter deposits. Individual fans within the blanket are flattened, with their long axes parallel to the margin-bounding faults, reflecting displacement along these faults. In contrast, very recent fans, separated from the older fan-apron deposits by a brief depositional break, are undeformed and preserve their original geometry. This contrast between the deformed fan-apron blanket and overlying undeformed recent fans demonstrates the ongoing activity of the faults controlling their deposition.

The sedimentary fill at the center of the Yedisu pull-apart basin consists of weakly lithified to loose, finer-grained sediments exposed along the axial plain (Figs. 4, 6, 7). They are composed of alternating finer-grained sandstone, laminated siltstone, mudstone, and claystone rich in organic material. Intercalations of cross-bedded sandstone to conglomerate lenses, ranging from 3 to 100 m in length, as well as localised peat occurrences, are also present. Vertical and lateral gradations are observed between the coarser-grained fan-apron deposits and the finer-grained depocenter facies. These sediments were transported and deposited by an antecedent drainage system, including the Perisuyu River and its major tributaries, within their channels and adjacent floodplains. Consequently, the lenticular Yedisu pull-apart basin and its undeformed Quaternary fill reflect a deformation history distinct from that of the surrounding faulted margins.

Active tectonics and related structures

Active tectonics is a scientific discipline that examines natural events on local to global scales over short geological time spans, ranging from a few seconds up to 2.588 My (Quaternary). Within this scope, earthquakes are key phenomena: they are rapid events lasting seconds to minutes, affecting areas ranging from a few to thousands of square kilometers. Active tectonics can therefore be viewed as the study of the short-term expression of neotectonic processes, including earthquakes, uplift, subsidence, creep, folding, and warping, tectonically driven sea-level changes, incision and offset of drainage systems, deformation and displacement of mainly alluvial-fan and fan-apron sediments, and Quaternary volcanic eruptions.

Seismicity of the Erzincan–Varto section

Historical earthquakes

The Erzincan–Varto section of the NAFS is characterised by a series of well-developed strike-slip complexities, including step-overs, bifurcation, bending, anastomosing patterns, and

pull-apart basins (Figs. 2, 5, 6). The intersection of two major shear zones (NAFS and EAFS), namely the Karlıova triple junction (KTJ), is also located in the same area. These structural complexities represent ideal sites for the accumulation of elastic strain energy due to the locking of motion along active fault segments. Consequently, the Erzincan–Varto section exhibits high seismicity, as evidenced by both seismic activity and historical earthquakes (Fig. 2; Tables 2, 3). Twelve destructive seismic events with intensities (I_0) ranging from VIII to X have been reported in the Erzincan–Varto section of the NAFS and its vicinity between AD 1045 and 1881 (Table 3).

These earthquakes resulted in loss of life, the destruction of thousands of structures, and the reactivation of the Nemrut volcano, which produced basaltic lava flows during the 1441 Bitlis–Muş–Van historical earthquake (Sieberg 1932; Salomon-Calvi 1940; Parejas et al. 1941; Pınar & Lahn 1952; Ergin et al. 1967; Wallace 1968; Karnik 1972; Can 1974; Ambraseys 1978, 2001, 2009; Toksöz et al. 1979; Soysal et al. 1981; Sipahioğlu 1982; Sipahioğlu & Alptekin 1988; Toksöz et al. 1988; Ambraseys & Finkel 1995; Stein et al. 1997; Ambraseys & Jackson 1998). In fact, there are no reliable data concerning key parameters of the historical earthquakes, such as the time of occurrence, site of epicentral locations, focal depth, magnitude, and source mechanism. Despite the poorly defined information on these historical events, the earthquake of 18 July 1784 stands out as particularly significant. It was the last seismic event in the region and is believed to have originated from the Uzunçayır master fault segment of the NAFS, located between the epicenters of the 1967 and 1992 earthquakes (Fig. 2). The earthquake rupture propagated both eastwards and westwards for approximately 100 km, between the epicenters of the 1949 Elmalı (Karlıova) and 1992 Yarbaşı (Pülümür) earthquakes (Fig. 2). This devastating event caused the loss of approximately 15,000 lives. The time elapsed since the 1784 Uzunçayır (Pülümür) historical earthquake is 241 years. According to GPS data, the average slip rate along the master fault of the NAFS within its Erzincan–Varto section ranges from 15 to 24 mm/yr (Reilinger et al. 1997, 2006; Kahle et al. 2000; McClusky et al. 2000). These values are consistent with the data obtained from field geological mapping conducted in and around the Yedisu pull-apart basin. There are well-established relationships among the slip rate, the recurrence interval between successive large earthquakes, the surface rupture length, the co-seismic slip, and the earthquake magnitude. Based on these relationships, co-seismic slip is estimated at 3.5–4.5 m. The amount of strain energy accumulated in the Uzunçayır (Yedisu) seismic gap (Fig. 2) since the 1784 event may therefore correspond to a future large earthquake with a magnitude of $M_w \geq 7.0$ (Wells & Coppersmith 1994).

Earthquakes in the period 1939–2020

Sixteen seismic events with magnitudes ranging from M_s 4.9 to M_s 7.9 have been reported from the Erzincan–Varto section of the NAFS and its vicinity during the instrumental period (events 2–16 in Table 2). The epicentral coordinates of these events indicate the presence of several active fault zones of differing characteristics in the region, although many of them were poorly defined. Among these, five major earthquakes were highly destructive, each followed by thousands of aftershocks. These earthquakes caused severe damage and resulted in significant loss of life throughout the region. They include the 26 December 1939 Koçyatağı (Erzincan), 8 August 1949 Elmalı, 19 August 1966 Sazlıca (Varto), 13 March 1992 Saztepe (Erzincan), and 22 January 2003 Pülümür earthquakes (events 2, 3, 5, 8, and 10 in Table 2). Among these, the 26 December 1939 Koçyatağı (Erzincan) earthquake is the largest seismic event sourced from the Karadağ master fault segment (Y-shear) of the dextral NAFS (Fig. 3). Its epicenter is located at the junction between the NW-trending NAFS and the E–W-trending Başköy–Kandilli fault zone (Fig. 1b). During this earthquake, a 360 km long surface rupture developed, with 12 m of right-lateral and 3.5 m of vertical displacement (Koçyiğit & Tokay 1985). The high elastic strain energy accumulated along the Erzincan–Varto section of the NAFS was released through earthquakes that occurred during the instrumental period. However, the Elmalı–Yarbaşı area, located in the central part of this section, has retained its character as a long-term seismic gap (241 years), despite the occurrence of an intermediate event; namely the 26 July 1967 Kabayel earthquake of (M_w 5.9), within the same area. Since the accumulated strain energy in this area is estimated to correspond to a potential seismic event of $M_w \geq 7.0$ (based on the slip rate and the time elapsed since the last destructive historical earthquake – the 1784 Uzunçayır earthquake), this area is referred to as the Tanyeri–Yedisu seismic gap in the present study (Wells & Coppersmith 1994). This segment might reactivate in the near future, posing a high seismic risk to the region.

Consequently, both the historical and instrumental period earthquakes strongly demonstrate the dominance of a strike-slip neotectonic regime in the Erzincan–Varto section of the NAFS

Table 3: Destructive historical earthquakes occurred in the Erzincan–Varto section of the NAFS.

No	Date	Intensity (I_o)	Number of casualties
12	1881	IX	
11	1784	IX	15,000
10	1667 or 1668	X	Half of the town was destroyed
9	1578	VIII	15,000
8	1458	X	32,000
7	1441	X	Nemrut volcano reactivated
6	1363	VIII	
5	1268	IX	15,000
4	1254 or 1255	VIII	16,000
3	1170	IX	
2	1168	VIII	12,000
1	1045	X–XI	

*These data were documented from the following works: Sieberg (1932), Ali (1932), Salomon-Calvi (1940), Parejas et al. (1941), Pınar & Lahn (1952), Ergin et al. (1967), Ambraseys (1978), Karnik (1972), Can (1974), Dewey (1976), Soysal et al. (1981), Sipahioğlu (1982), Guidoboni et al. (1994), Ambraseys & Finkel (1995), Guidoboni & Comastri (2005).

and its surrounding area. Furthermore, focal mechanism solutions of the instrumental period earthquakes are consistent with the regional stress regime, in which the maximum (σ_1), intermediate (σ_2) and minimum (σ_3) principal stress axes are oriented in approximately the horizontal (N–S), vertical, and horizontal (E–W) directions, respectively (Fig. 1b).

Yedisu pull-apart basin

This is an approximately 0.5–4-km-wide, 12-km-long, WNW-trending and actively growing strike-slip depression developed along the master fault segment (Y-shear) of the NAFS. It reaches its maximum width (4 km) in the central part (Fig. 7) and gradually narrows and pinches out towards both its western and eastern terminations, resulting in a lenticular shape (Figs. 2, 5, 6a). The Yedisu pull-apart basin is bounded by several structural highlands, including the Şeytan Mountains to the south, with a highest peak of 2630 m asl, and a series of hills rising to 1827 m asl along its northern margin. The elevation of the basin floor ranges from 1428 m asl at the center and 1360 m asl at its westernmost tip. Consequently, the maximum relief between the basin floor and the surrounding highlands is approximately 1270 m to the south and 467 m asl to the north, indicating that the tectono-morphology of the basin is asymmetric. The Yedisu pull-apart basin is drained by the Perisuyu River and its numerous transverse tributaries (Fig. 6a). The Perisuyu River enters the basin at its eastern margin, flows WNW along its entire length, then bends south and exits the basin (Fig. 5). The basin continues to develop on the erosional surface of the Upper Cretaceous ophiolitic mélange and its forearc cover sequence, which were formed and derived from both the northern Neo-Tethys and the Inner Tauride oceans, under the control of a strike-slip neotectonic regime since the Early Quaternary (c. 2.588 Myr) (Fig. 6).

Faults

Starting approximately from the east of the Tanyeri settlement, the NAFS bifurcates into several fault zones and individual fault segments, including the Perisuyu, Kızılçubuk, and Yeşilgöl fault zones (Fig. 5). The recognition of these faults was based on, a series of structural and morphotectonic markers, such as earthquakes, slickensides, deflected to offset drainage systems, displaced rock unit boundaries, tectonic juxtaposition of older rocks with Quaternary deposits, alignment of older and recent alluvial fans, deformed and offset fans, abrupt slope breaks, back-tilting of blocks, and uplifted to dissected Pleistocene to recent terrace deposits, among others. The major fault zones, fault segments, and their diagnostic characteristics are described in detail below.

Perisuyu fault zone

The Perisuyu fault zone is located to the east of the Tanyeri settlement in the WNW and extends to the Yukarı Sarıkuşak–Kızılçubuk villages in the ESE. Its general outcrop pattern is anastomosing and includes the master fault of the NAFS (Fig. 2). The Perisuyu drainage system is controlled by the Tanyeri–Yeni Sarıkuşak section of the NAFS; therefore, this section is referred to as the Perisuyu fault zone in the present study. It is approximately 0.1–6 km wide, 105 km long, and generally WNW-trending. Based on its general trend, the zone can be divided into two major sections: (1) WNW-trending, 73 km long Tanyeri–Elmalı section, which also represents the long-term seismic gap and is the focus of the present study. (2) NE-trending, 32 km long Elmalı–Yeni Sarıkuşak section (Figs. 2, 5). Near Gelinpertek, the Perisuyu fault zone bifurcates into several fault segments, resulting in an intervening depression, namely the Yedisu pull-apart basin (Figs. 5 and last 7). These fault segments converge towards the ESE, where the Yedisu pull-apart basin narrows and terminate (Figs. 5, 6, 7). The two-dimensional pattern of the fault segments taking part in the development of the Yedisu pull-apart basin is well illustrated in Figs. 6 and 7.

The Elmalı–Yeni Sarıkuşak section of the Perisuyu fault zone is an approximately 2 km wide, 32 km long, ENE-trending zone of strike-slip faulting. Near Elmalı settlement, the fault zone bends left, bifurcates into two strands, and forms a pressure ridge, referred to as the Elmalı pressure ridge. This structural complexity also marks the WSW tip of the Elmalı–Yukarıkuşak section of the Perisuyu fault zone (Figs. 5 and 8). This pressure ridge pinches out near the eastern margin of the Aktaş settlement, after which the fault zone continues as two closely-spaced, parallel strands for approximately 4 km up to the İsmail Komu (Fig. 8). Starting from the İsmail Komu, the Perisuyu fault zone rebifurcates into three strands, from north to south, which are the Kuşakdere, Kom, and Kaynarpınar strands, respectively. One of the major tributaries of the Perisuyu River, the Kuşak Stream, is controlled and offset by the Kuşakdere faults. The other two strands represent the master faults, which also control and offset the Perisuyu River (Fig. 8). Additionally, the Kuşakdere fault segment bends northward, forming a second pressure ridge, referred to as the Kom pressure ridge (Fig. 8). In the Yeni Sarıkuşak and Kızılçubuk area, the ENE-trending Perisuyu fault zone (Elmalı–Yeni Sarıkuşak section) is dextrally offset by the NW-trending Kızılçubuk fault zone (Fig. 8). Beyond this, the fault zone, continues as both the Kaşıkçı and Dörtyol (Çatak) faults, along with the intervening Kaşıkçı pull-apart basin (Fig. 5). The Elmalı–Yeni Sarıkuşak section of the Perisuyu fault zone comprises numerous fault segments of varying trends and lengths, which are 0.7–11 km long, parallel to sub-parallel, closely spaced (0.6–2 km), and exhibit a well-developed anastomosing faulting pattern (Fig. 8). Some of these fault segments display well-developed and preserved slickensides at stations S1 and S2 (Fig. 8).

Kinematic analysis of slip-plane data measured at station S1 indicates that this fault segment is an oblique-slip reverse fault. In contrast, kinematic analysis of the slip-plane data obtained from station S2 shows that the fault segment is a dextral strike-slip fault, resulting from the principal compressive stress

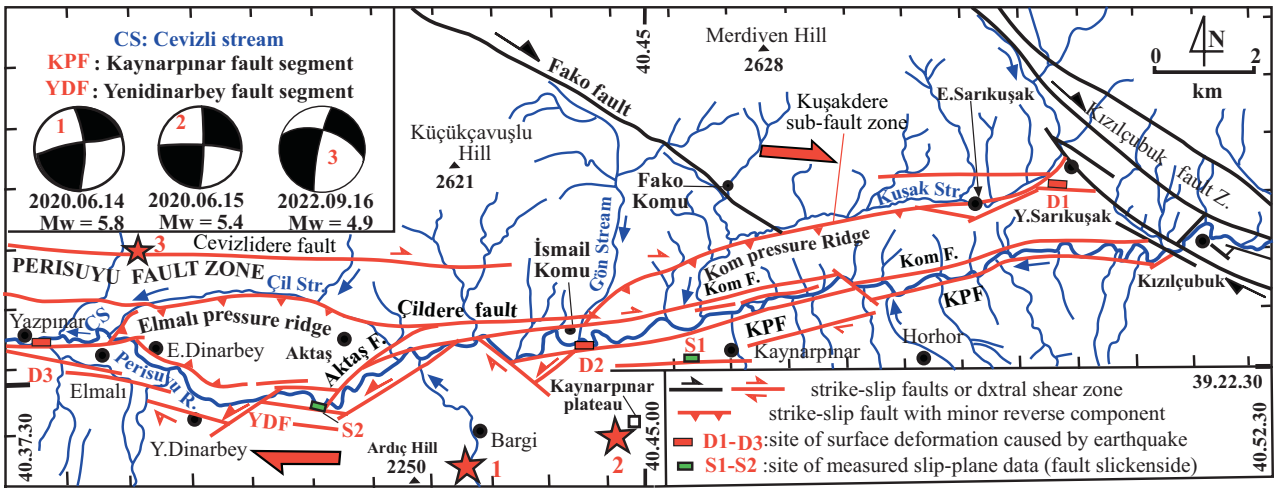

Fig. 8. Seismotectonic map of the eastern section of the Perisuyu fault zone (focal mechanism solutions from ERD 2023).

oriented in NNW–SSE (Fig. 9). In addition, the Kuşakdere fault is not a single fault but, rather, a sub-fault zone. It bifurcates into several fault segments, exhibiting both relay and anastomosing faulting patterns (Fig. 10). The eastern tip of the Elmalı pressure ridge and the Perisuyu River are being bounded and controlled by the NE-trending Aktaş faults, which have cut and uplifted older river deposits by up to 40 m (Figs. 8, 11). Similarly, the Perisuyu River is controlled by the Kom faults, the master strands of the Perisuyu fault zone. Here, older river deposits and point-bar clastics have also been cut and uplifted as fault-suspended terrace deposits by the Kom faults (T1 and T2 in Fig. 12). The eastern section of the Perisuyu fault zone Elmalı–Sarıkuşak section) was reactivated by several seismic events, including M_w 6.5 1949 Elmalı, M_w 5.7 2005 Kızılçubuk, M_w 5.8 and 5.6 2020 Bargi Kaynarpınar Plateau, and M_w 4.9 2022 Cevizlidere earthquakes (Figs. 2, 8). These earthquakes (1, 2 and 3 in Fig. 8) also produced ground ruptures due to their very shallow hypocenters (D1, D2 and D3 in Figs. 8, 13). The Cevizlidere earthquake (3 in Fig. 8) originated from the Cevizlidere fault, while both the Bargi and Kaynarpınar earthquakes (1 and 2 in Fig. 8) were likely sourced from the Kom fault segments (Figs. 8, 12).

Kızılçubuk Fault Zone

In general, the Kızılçubuk Fault is 0.2–10 km wide, approximately 110 km long, and WNW-trending, representing a dextral strike-slip fault zone. It extends from near the southeast of Varto in the east to near the northeast of Yağmurdere settlement in the northwest (Figs. 2, 5, 8). One of the most diagnostic geomorphic markers demonstrating

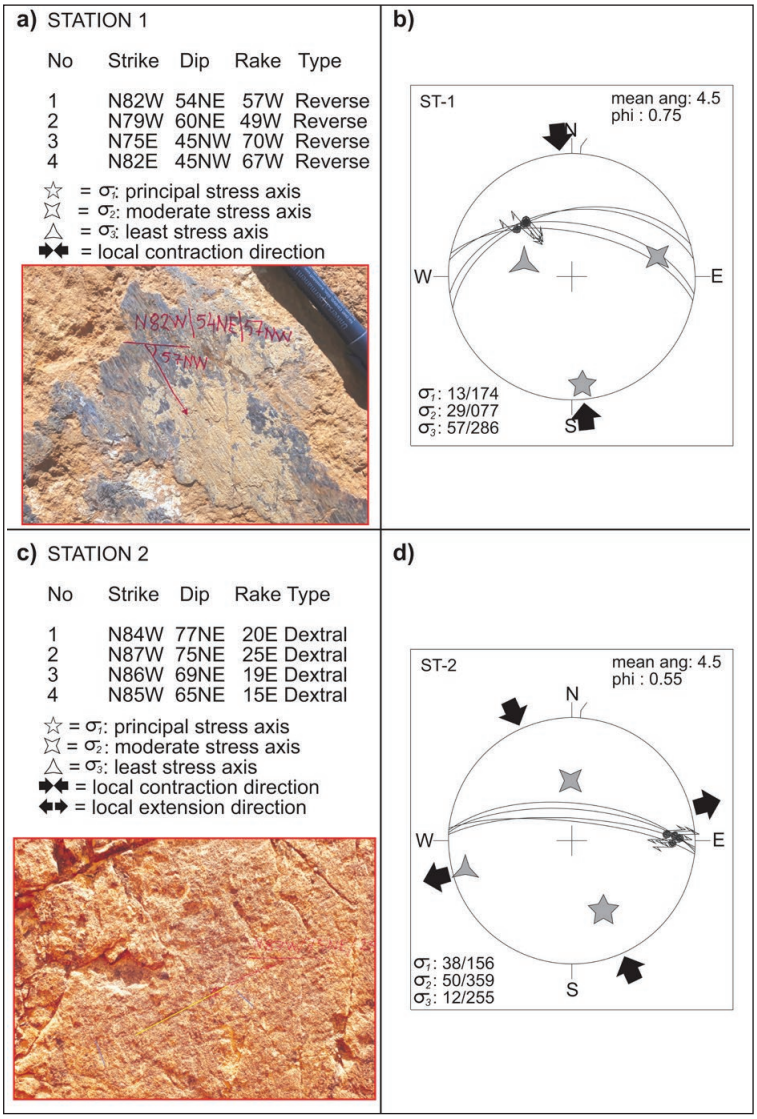

Fig. 9. Slip-planes (Slickensides) determined at stations S1–S2 in Fig. 8, measured slip planes data and their kinematic analysis.

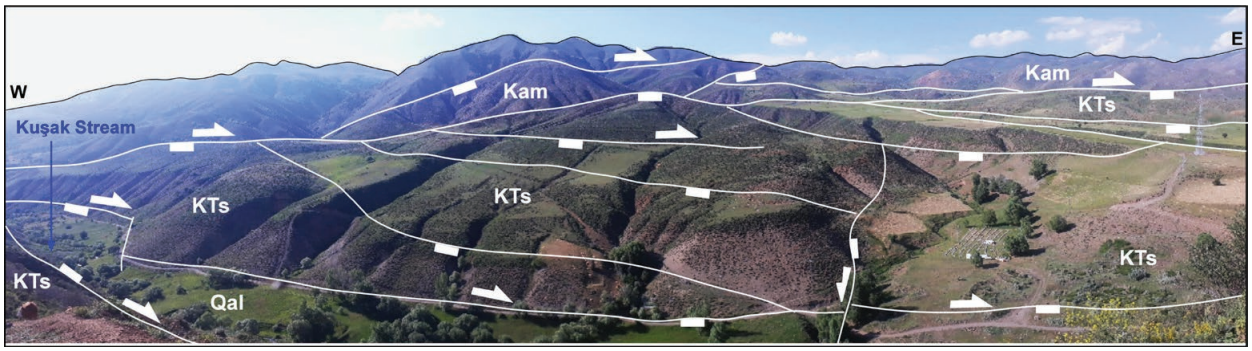

Fig. 10. Field photograph illustrating the Kuşakdere sub-fault zone and its anastomosing and relay faulting pattern (view to WNW). Kam – Anatolian Nappe of late Cretaceous age, KTs – Sütpınar Formation of Campanian-Paleocene age, Qal – Quaternary alluvial deposits.

Fig. 11. Field photograph illustrating NE trending Aktaş fault scarp controlling the Perisuyu River and 40 m uplifted river terrace deposits (view to WNW). KTs – Sütpınar Formation of Campanian–Paleocene age, F1, F2, F3, and F4 are faults in the order of ages.

both the existence and activity of the Kızılçubuk fault zone, is the fault-controlled (deflected and offset) drainage system, such as the Perisuyu River and its numerous first-, second-, and third-order tributaries. For example, the main channel of the Perisuyu River is offset by up to 12 km in a dextral direction (Fig. 5). Similarly, around the Başköy pull-apart basin, Miocene marine limestone and fluvial clastic rocks are cut and offset by up to 10 km in a dextral sense (Fig. 5). In addition, the Kızılçubuk fault zone was reactivated by several seismic events, including M_w 6.8 (1966) Sazlıca, M_w 5.7 (1966) Güzeldere, M_w 5.9 (2005) Ilıpınar and M_w 5.7 (2005) Kızılçubuk earthquakes (Table 2, Fig. 2).

Yeşilgöl Fault Zone

The Yeşilgöl fault zone is approximately 0.5–3 km wide, 30 km long, and NE-trending, representing a sinistral strike-slip fault zone. It extends from near the east of Başköy in the northeast to the Ekşipınar settlement in the southwest (Fig. 5). Along its entire length, various rock units, including the colored ophiolitic mélange (Anatolian nappe: Kam), the Sütpınar Formation (KTs), and Miocene carbonates and fluvial clastic rocks are cut, displaced by up to 18 km, and tectonically juxtaposed with Quaternary alluvial deposits (Fig. 5). The Yeşilgöl fault zone forms the conjugate structure of

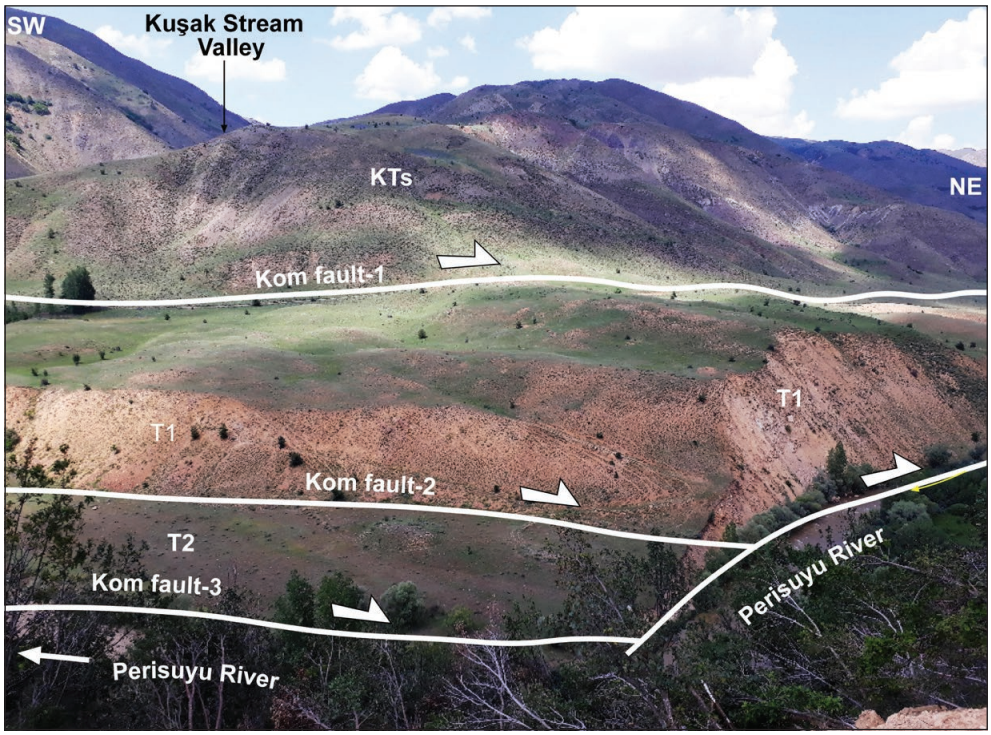

Fig. 12. Field photograph illustrating Kom faults and uplifted terraces (T1 and T2) (view to NNW). KTs – Sütpınar Formation of Campanian–Paleocene age.

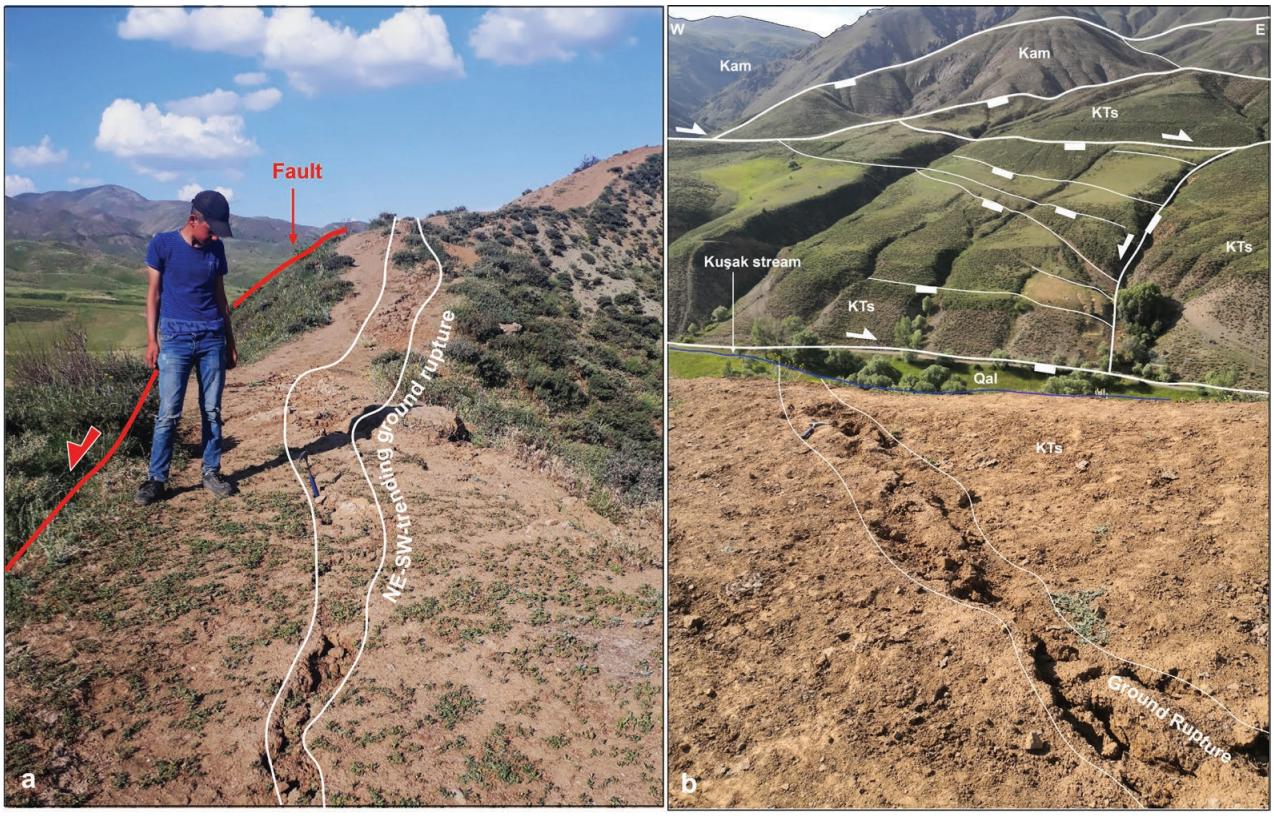

Fig. 13. (a) Field photograph illustrating the general view of the Sarıkuşak ground rupture at D1; **(b)** Field photograph illustrating both the Sarıkuşak sub-fault zone (in background) and the ground rupture (in foreground) at D1 in Fig. 8 (view to NNW). Kam – Anatolian Nappe of late Cretaceous age, KTs – Sütpınar Formation of Campanian–Paleocene age, Qal – Quaternary alluvial deposits.

the Kızılçubuk fault zone, together forming the Başköy pull-apart basin. Its activity is evidenced by the kinematic relationship with the Kızılçubuk fault zone and the tectonic juxtaposition of Quaternary alluvial deposits with older rocks.

Results
(age, total displacement, slip rate and return period)

From a tectonic perspective, the study area is located at the western tip of the East Anatolian Tectonic Block (EATB) (Koçyiğit 2023), along the Erzincan–Varto section of the NAFS (Fig. 1). Doming of the Precambrian African Shield began along a NW–SE-trending elongated zone during the Late Cretaceous–Eocene (Al-Saad & İbrahim 2002). This doming generated NE–SW oriented extensional stresses (Madanipour et al. 2024), which induced NW-trending normal step faults and associated rifting along this mega-crack during the late Eocene–Oligocene. Thus, Arabia began to separate from Africa. However, this separation and the north-northeastward motion of Arabia (Strohmenger & Jameson 2015) slowed and eventually ceased due to the final cessation of subduction of the Arabian plate beneath eastern Türkiye and southwestern Iran, i.e., along the Bitlis–Zagros Suture Zone during the Early–Middle Miocene (Burdigalian–Serravallian) (Hempton 1987).

During the latest Miocene–Pliocene, seafloor spreading along the Red Sea commenced (Hempton 1987), reactivating the slow northward motion of the Arabian Plate. Additionally, at the beginning of the Quaternary (~2.6 My), two major intra-continental strike-slip fault systems, the dextral NAFS and sinistral EAFS, formed (Fig. 1), initiating the west-southwestward motion of the intervening Anatolian platelet, which started to move in a west-southwest direction (Koçyiğit et al. 2001; Aksoy et al. 2007; Çolak et al. 2012; Koçyiğit 2013; Gürboğa 2015; Koçyiğit & Canoğlu 2017). This event accelerated the northward motion of the Arabian Plate. Consequently, the onset age of the NAFS is not Late Middle Miocene, but rather, Early Quaternary (Hempton 1987; Aksoy et al. 2007; Çolak et al. 2012; Koçyiğit 2013).

Around the Erzincan pull-apart basin, the Inner Tauride Suture (ITS) is cut and displaced up to 62 km dextrally by the NAFS (A–B=62 km in Fig. 2). In the same area, the Fırat River is controlled and offset up to 68 km dextrally by the NAFS (X–Y=68 km in Fig. 2). Similarly, in the Yedisu–Kaşıkçı area, the main course of the Yedisu River is offset up to 55 km dextrally by the Yedisu and Kızılçubuk fault zones, which comprise the eastern section of the NAFS (A–B=55 km in Fig. 5). In this area as well, the boundary of the Upper Cretaceous Anatolian Nappe (Kam) is cut and displaced up to 41 km dextrally by the eastern section of the NAFS (X–Y= 41 km in Fig. 5).

Based on both structural and geomorphic markers, the total average dextral displacement accumulated along the eastern section of the NAFS is approximately 57 km. This total offset was accumulated over a time span of about 2.588 Myr, corresponding to an average uniform slip rate of 22 mm/yr. The average slip rate on the master fault of the NAFS within its Erzincan–Varto section ranges from 15 to 24 mm/yr, as indicated by GPS data (Reilinger et al.1997, 2006; Kahle et al. 2000; McClusky et al. 2000). Therefore, our calculated value agrees well with the geodetic data.

Based on this average slip rate (22 mm/yr), the recurrence interval of a large earthquake with a magnitude $M_w \geq 7.0$ for the eastern section of the NAFS is estimated at approximately 205±50 years. The last major destructive earthquake in this area, the 1784 Uzunçayır–Yedisu earthquake (Fig. 2), occurred 241 years ago (Ambrasyes 1978; Ambrasyes & Jackson 1998). Consequently, a new peak earthquake of $M_w \geq 7.0$ may occur at any time in the near future, i.e. the Tanyeri–Yedisu seismic gap (Fig. 1) will be reactivated. In contrast to our result, the lengths of the return periods of $M_w \geq 7.0$ peak earthquakes to be sourced from the eastern section of the NAFS were determined based on paleoseismological studies carried out on the Ilısu fault by Sançar & Akyüz (2014). According to these authors, the return periods vary from 1660 to 4220 years. However, this result is highly improbable, as there is a significant contradiction between these long return periods and the uniform slip rate on the Ilısu fault (Fig. 14).

Discussion

Based on historical earthquake records (Ambraseys 2009), the most recent event on this segment is reported to have occurred in 1784 (Okumura 1994). The first comprehensive study using trenching paleoseismology was applied by Okumura (1994) in the Erzincan Basin. It was determined that five paleoearthquakes occurred based on a precise stratigraphic chronology. According to the results of this study, an average recurrence interval is approximately suggested 200 to 250 years for the area (Okumura 1994; Fraser et al. 2010a,b). Moreover, recurrence interval along the Refahiye segment, located on the western part of the Tanyeri–Yedisu segment is determined to be between 200–900 years (Hartleb et al. 2003; Gürboğa & Gökçe 2019). The Tanyeri–Yedisu segment, which is classified as a seismic gap (Okumura 1994; Zapcı et al. 2017; Sünbül 2025), did not rupture during the recent earthquake sequence; in addition, about 241 years have elapsed since the last major event and the NAFS accommodates an average slip rate of about 20 mm/yr. The localized concentration of crustal shortening coincides with elevated Coulomb stress accumulation, pronounced GPS velocity gradients, and historical seismic quiescence (Sünbül 2019, 2025). In accordance with another GPS and seismicity approach, the accumulated slip deficit is about 2.67 m and a high accumulation of strain proved by b-values point out that there is an earthquake potential up to M_w 7.5 sourced from the entire segment with a slip rate of more than 11 mm/yr (Aktug et al. 2013).

Collectively, these observations indicate that the Tanyeri–Yedisu segment is not merely a geometrically segmented portion of the fault, but also a mechanically strong and highly

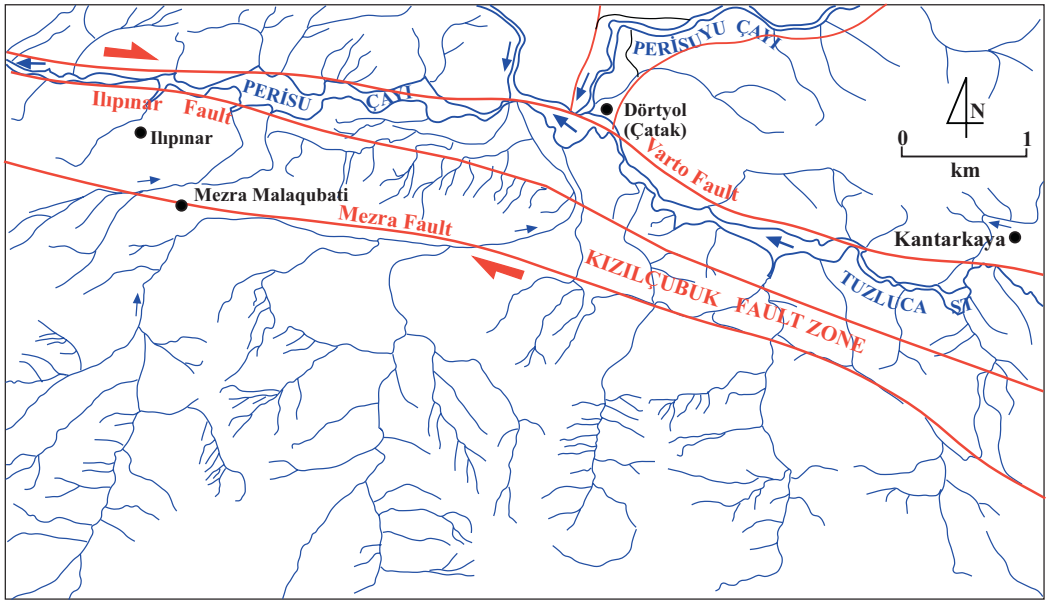

Fig. 14. Simplified Kızılçubuk neotectonic map illustrating the relationship between the active faults and the fault-controlled (deflected to offset) drainage system (Perisuyu River).

locked structure. Taken together, these factors clearly suggest that the probability of rupture on this segment is currently very high.

In conclusion, the onset of the prominent strike-slip neotectonic regime in the region, and the development of its associated structural elements – most notably the Anatolian platelet and its major margin-bounding fault systems, the NAFS and the EAFS – are constrained to the Early Quaternary. This result is supported by the field geological data regarding various deformation patterns of different rock assemblages and sedimentary deposits. Within this framework, the Erzincan–Varto section of the NAFS has accommodated a cumulative, nearly uniform dextral strike-slip displacement of about 57 km, implying a long-term, uniform slip rate on this segment of approximately 22 mm/yr. When these kinematic estimates are integrated with seismic hazard assessments, they indicate that the recurrence interval of $M_w \geq 7.0$ earthquakes sourced from the Tanyeri–Yedisu seismic gap is on the order of 205±50 years. Given this characteristic timescale, the long-lived Tanyeri–Yedisu seismic gap, which has not produced a major event for more than one full recurrence cycle, is considered capable of reactivating at any time in the near future and thus represents a locus of significantly elevated seismic risk for the region.

Conclusions

Based on the presented in the preceding sections, the following conclusions may be drawn:

- The onset of the prominent strike-slip neotectonic regime, alongside the formation of associated structures – specifically the Anatolian platelet and its margin-bounding faults (the NAFS and EAFS), occurred during the Early Quaternary.
- The total uniform dextral strike-slip displacement accumulated along the Erzincan–Varto section of the NAFS is 57 km.
- The uniform slip rate along the Erzincan–Varto section of the NAFS is estimated at approximately 22 mm/yr.
- The return period of a peak earthquake of $M_w \geq 7.0$ originating from the Tanyeri–Yedisu seismic gap is 205±50 years.
- The long-standing Tanyeri–Yedisu seismic gap might reactivate in the near future, posing a significant seismic risk to the region.

References

Aksoy E., İnceöz M. & Koçyiğit A. 2007: Lake Hazar basin: a negative flower structure on the East Anatolian fault system (EAFS), SE Turkiye. *Turkish Journal of Earth Sciences* 16, 319–338.

Aktug B., Dikmen U., Dogru A. & Ozener H. 2013: Seismicity and strain accumulation around Karliova triple junction (Turkey). *Journal of Geodynamics* 67, 21–29. https://doi.org/10.1016/j.jog.2012.04.008

Al-Saad H. & Ibrahim M.I. 2002: Stratigraphy, micropaleontology, and paleoecology of the Miocene Dam Formation, Qatar. *GeoArabia* 7, 9–28.

Ali K. 1932: Erzincan Earthquakes. In: *Erzincan province year-book*, 110–115.

Ambraseys N.N. 1978: *Studies in historical seismicity and tectonics, Geodynamics of Today*. The Royal Society London, 7–16.

Ambraseys N.N. 2001: Reassessment of earthquakes, 1900–1999, in the Eastern Mediterranean and the Middle East. *Geophysical Journal International* 145, 471–485. https://doi.org/10.1046/j.0956-540x.2001.01396.x

Ambraseys N. 2009: *Earthquakes in the Mediterranean and Middle East: a multidisciplinary study of seismicity up to 1900*. Cam-

bridge University Press. https://doi.org/10.1017/CBO9781139195430.004

Ambraseys N.N. & Finkel C. 1995: *The Seismicity of Turkey and Adjacent Areas 1500–1800*. Eren Publishers, Istanbul.

Ambraseys N.N. & Jackson J.A. 1998: Faulting associated with historical and recent earthquakes in the eastern Mediterranean region. *Geophysical Journal of Intitudes* 133, 390–406.

Can R. 1974: *Seismotectonics of the North Anatolian Fault Zone*. Unpublished M. Phil, thesis. University of London.

Çolak S., Aksoy E., Koçyiğit A. & Inceöz M. 2012: Palu-Uluova strike-slip basin on the East Anatolian Fault System, Turkey: transition from paleotectonic period to neotectonic period. *Turkish Journal Earth Sciences* 21, 547–570.

Dewey J.F. 1976: Ophiolite obduction. *Tectonophysics* 31, 93–120. https://doi.org/10.1016/0040-1951(76)90169-4

ERD (AFAD) 2000, 2020, 2023: Disaster and Emergency Management Presidency, Earthquake Research Department. Web page: http://www.deprem.gov.tr/Sarbis/Shared/Anasayfa.aspx

Ergin K., Güçlü U. & Uz Z. 1967: A catalogue of earthquakes for Turkey and surrounding area (11 AD to 1964 AD). *Tech. Univ. Mining Eng. Fac. Publ.* 24, 74.

Eyidoğan H. 1992: 13 Mart 1992 Erzincan depreminin ana şok ve art sarsıntı özellikleri üzerine bir tartışma. *Jeofizik* 6, 103–112.

Eyidoğan H., Güçlü U., Utku Z. & Değirmenci E. 1991: *Türkiye Büyük Depremleri Makrosismik Rehberi (1900–1988)* [A Macroseismic Guide for the Earthquakes of Turkey]. İstanbul Technical University (in Turkish).

Fraser J., Hubert-Ferrari A., Vanneste K., Altinok S., Drab L. 2010a: A relict paleoseismic record of seven earthquakes between 2000 B.C. and 600 A.D. on the central North Anatolian fault at Elmacik, near Osmancik, Turkey. *GSA Bulletin* 122, 1830–1845. https://doi.org/10.1130/B30081.1

Fraser J., Vanneste K. & Hubert-Ferrari A. 2010b: Recent behavior of the North Anatolian Fault: Insights from an integrated paleoseismological data set. *Journal of Geophysical Research Solid Earth* 115, B09316. https://doi.org/10.1029/2009JB006982

Guidoboni E. & Comastri A. 2005: *Catalogues of Earthquakes and Tsunamis in the Mediterranean Area from the 11th to 15th Century*. Instituto Nazionale di Geofisica e Vulcanologia, Rome.

Guidoboni E., Comastri A. & Traina G. 1994: *Catalogue of ancient earthquakes in the Mediterranean area up to the 10th century*. Vol. 1, ING-SGA, Bologna, 1–504.

Gürboğa Ş. 2015: Source fault of 19 August 1966 Varto earthquake and its' mechanism: New field data, Eastern Turkey. *Journal of Asian Earth Sciences* 111(4), 792–803.

Gürboğa Ş. & Gökçe O. 2019: Paleoseismological catalog of Pre-2012 trench studies on the active faults in Turkey. *Bulletin of Mineral Research and Exploration* 159, 63–87. https://doi.org/10.19111/bulletinofmre.561925

Hartleb R.D., Dolan J.F., Akyüz H.S. & Yerli B. 2003: A 2000-year-long paleoseismologic record of earthquakes along the central North Anatolian Fault, from trenches at Alayurt, Turkey. *Bulletin of the Seismological Society of America* 93, 1935–1954. https://doi.org/10.1785/0120010271

HARVARD 2004: *Harvard University, Harvard Seismology Group, CMT catalogue*. Web page: http://www.seismology.harvard.edu

Hempton M.R. 1987: Constraints on Arabian plate motion and extensional history of the Red Sea. *Tectonics* 6, 687–705.

Irmak S., Doğan B. & Karakaş A. 2012: Source mechanism of the 23 October, 2011, Van (Turkey) earthquake (Mw =7.1) and aftershocks with its tectonic implications. *Earth Planets Space* 64, 991–1003. https://doi.org/10.5047/eps.2012.05.002

Kahle H.G., Cocard M., Peter Y., Geiger A., Reilinger R., Barka A. & Veis G. 2000: GPS-derived strain rate field within the boundary zone of the Eurasian, African and Arabian plates. *Journal of Geophysical Research* 105, 23353–23370.

Kalafat D., Günes Y., Kekovalı K., Kara M., Deniz P. & Yılmazer M. 2011: *A Revised and Extented Earthquake Cataloque for Turkey since 1900 (M ≥ 4.0)*. Boğaziçi University, Kandilli Observatory and Earthquake Research Institute, İstanbul.

Karnik V. 1972: *Seismicity of the Evropean area*. Part 2. Reidel, Dordrecht.

Koçyiğit A. 1983: The seismicity of the eastern Anatolia region and required studies. *The Earth and Human* 8, 25–29.

Koçyiğit A. 1989: Suşehri basin: an active fault-wedge basin on the North Anatolian Fault Zone, Turkey. *Tectonophysics* 167, 13–29.

Koçyiğit A. 1990: Tectonic setting of the Gölova basin: Total offset of the North Anatolian fault zone, E Pontides, Turkey. *Annales Tectonicae* IV, 155–170.

Koçyiğit A. 1991: An example of an accretionary fore-arc basin from northern Central Anatolia and its implications for the history of Neo-Tethys in Turkey. *Geological Society of America Bulletin* 103, 22–36.

Koçyiğit A. 2013: New field and seismic data about the intraplate strike-slip deformation in Van region, East Anatolian plateau, E. Turkey. *Journal of Asian Earth Sciences* 62, 586–605. https://doi.org/10.1016/j.jseaes.2012.11.008

Koçyiğit A. 2023: Neotectonic and geothermel potantial of the East Anatolian Tectonic Block: A case study in Diyadin (Ağrı) geothermal field. *Bulletin of the Mineral Research and Exploration* 171, 33–68. https://doi.org/10.19111/bulletinofmre.1248712

Koçyiğit, A. & Canoğlu, C. 2017: Neotectonics and seismicity of the Erzurum pull-apart basin, East Turkey. *Russian Geology and Geophysics* 58, 99–122.

Koçyiğit A. & Tokay M. 1985: Çatalçam (Zevker)–Erzincan arasinda Kuzey Anadolu Fay Kusagi'nin sismo-tektonik incelemesi: Fay kusaginin tek tono-stratigrafisi, sistematigi ve neotektonik özellikleri. *Bayindirlik ve Iskan Bakanligi Teknik Arastirma ve Uygulama Genel Müdürlügü*, Proje Report No. 82-04-08-00-02, 1–101.

Koçyiğit A., Yilmaz A., Adamia S. & Kuloshvili S. 2001: Neotectonic of East Anatolian Plateau (Turkey) and Lesser Caucasus: Implication for transition from thrusting to strike-slip faulting. *Geodinamica Acta* 14, 177–195. https://doi.org/10.1016/S0985-3111(00)01064-0

KOERİ 2011, 2020, 2022: Kandilli Observatory and Earthquake Research Institute. National earthquake monitorin center catalogue. http://www.koeri.boun.edu.tr

Madanipour S., Najafi M., Nozaem R., Vergés J., Yassaghi A., Heydari I., Sedigheh T., Khodaparast S., Soudmand Z. & Aghajari L. 2024: The Arabia–Eurasia collision zone in Iran: Tectonostratigraphic and structural synthesis. *Journal of Petroleum Geology* 47, 445–504. https://doi.org/10.1111/jpg.12854

McClusky S., Balassanian S., Barka A., Demir C., Engintav S., Georgiev I., Gürkan O., Hamburgor M., Hurst K., Kahle H., Kastens K., Kekelidze G., Kink R., Kotzev V., Lenk O., Mahmoud S., Mishin A., Nadariya M., Ouzounis A., Paradissis D., Peter Y., Prilepin M., Reiling R., Sanlı I., Seeger H., Tealeb A., Toksöz N.M. & Jeis G. 2000: Global positioning system constraints on plate kinematics and dynamics in the eastern Mediterranean and Caucasus. *Journal of Geophysical Research* 105, 5695–5719.

Okumura K., Yoshioka T., Kuşçu İ., Nakamura T. & Suzuki Y. 1994: *Recent surface faulting on the North Anatolian Fault East of Erzincan Basin, Turkey – a trenching survey*. Summaries of Researches using AMS at Nagoya University, 32–48 (in Japanese with English abstract).

Parejas E., Akyol I.H. & Altınlı E. 1941: Le tremblement de terre d'Erzincan du 27 Décembre 1939. *Revue Fac. Sei. Univ. Istanbul BVİ*, 177–222.

Pınar N. & Lahn E. 1952: *Turkish Earthquake Catalog with Descriptions*. Technical Report, Turkey. The Ministry of Public Works and Settlement. The General Directorate of Construction Affairs, Serial 6, No. 36.

Reilinger R.E., McClusky S.C., Oral M.B., King W. & Toksöz N. 1997: Global positioning system measurements of present-day crustal movements in the Arabia–Africa–Eurasia plate collision zone. *Journal of Geophysical Research Solid Earth* 102, 9983–9999. https://doi.org/10.1029/96JB03736

Reilinger R., McClusky S., Vernant P., Lawrance S., Ergintav S., Çakmak R., Özener H., Kadirov F., Guliev I., Stepanyan R., Nadariya M., Hahubia G., Mahmoud S., Sakr K., ArRajehi A., Paradissis D., Aydrus A., Prilepin M., Guseva T., Evren E., Dmitrotsa A., Filikov S., Gomez F., Ghazzi R. & Karam G. 2006: GPS constraints on continental deformation in the Africa–Arabia–Eurasia continental collision zone and implications for the dynamics of plate interactions. *Journal of Geophysical Research* 111, B05411. https://doi.org/10.1029/2005JB004051

Salomon-Calvi W. 1940: Anadolunun Teknotik Bünyesi Hakkındaki Almanca Tezin Bir Hülâsası. *Bulletin of the Mineral Research and Exploration* 18, 30–34.

Sançar T. & Akyüz H.S. 2014: Kuzey Anadolu Fay Zonu, Ilıpınar Segmenti'nin (Karlıova–Bingöl) Paleosismolojisi [Paleoseismology of the Ilıpınar Segment (Karlıova, Bingöl), The North Anatolian Fault Zone]. *Geological Bulletin of Turkey* 57, 35–51. https://doi.org/10.25288/tjb.298727

Şaroğlu F. & Yılmaz Y. 1986: Doğu Anadolu'da neotektonik dönemdeki jeolojik evrim ve havza modelleri. *Bulletin of the Mineral Research and Exploration* 107, 73–94.

Sieberg A. 1932: Untersuchungen über Erdbeben und Bruchschollenbau im oestlichen Mittelmeergebiet. *Denkschriften der medizinisch naturwissenschaftlichen Gesselschaft zu Jena* 18, 159–273.

Sipahioğlu S. 1982: *Seismo-tectonic features of the North Anatolian fault zone*. Ph. D. Thesis, Ist. univ. Fen Fak. Jeofizik B8l., 1–169.

Sipahioğlu S. & Alptekin Ö. 1988: Türkiye'de deprem sorununun görünümü. *Jeofizik* 2, 151–183.

Soysal H., Sipahioğlu S., Koçak D. & Altınok Y. 1981: *Historical Earthquake Catalogue of Turkey and Surrounding Area (2100 B.C.–1900 A.D.)*. İstanbul Univ., Department of Geophysics, Technical Report, TÜBITAK, No. TBAG-341.

Stein R.S., Barka A.A. & Dieterich J.H. 1997: Progressive failure on the North Anatolian fault since 1939 by earthquake stress triggering. *Geophysical Journal International* 128, 594–604. https://doi.org/10.1111/j.1365-246X.1997.tb05321.x

Strohmenger C.J. & Jameson J. 2015: Modern coastal systems of Qatar as analogues for arid climate carbonate reservoirs: improving geological and reservoir modelling. *First Break* 33, 41–50. https://doi.org/10.3997/1365-2397.2014027

Sünbül F. 2019: Time-dependent stress increase along the major faults in eastern Turkey. *Journal of Geodynamics* 126, 23–31. https://doi.org/10.1016/j.jog.2019.03.001

Sünbül F. 2025: Kuzey Anadolu Fayı Yedisu Segmenti Kabuk Deformasyon Analizi: GPS ve Sismolojik Veriler ile Entegratif Modelleme. *Geomatik* 11, 194–205.

Tan O.M., Tapırdamaz M.C. & Yörük A. 2008: The earthquake catalogues for Turkey. *Turkish Journal of Earth Sciences* 17, 405–418.

Tarhan N. 1991: Hınıs–Varto–Karlıova (Erzurum–Muş–Bingöl) dolayındaki neojen volkanit-lerinin jeolojisi ve petrolojisi. *Bulletin of the Mineral Research and Exploration* 113, 45–60.

Toksöz M.N., Arpat E. & Şaroğlu F. 1977: East Anatolian Earthquake of 24 November 1976. *Nature* 270, 423–425.

Toksöz M.N., Shakal A.F. & Michael S.J. 1979: Space-time migration of earthquakes along the North Anatolian fault zone and seismic gaps. *Pure and Applied Geophysics* 117, 1258–1269.

Toksöz M.N., Guenette M., Gülen L., Keough G., Pulli J.J., Sav H. & Olguner A. 1983: Source mechanism of Narman–Horasan earthquake. *Yeryuvarı ve İnsan* 8, 47–52.

Toksöz M.N., Dainty A.M., Reiter E. & Wu R.S. 1988: A model for attenuation and scattering in the earth's crust. *Pure and Applied Geophysics* 128, 81–100.

Tutkun S.Z. & Hancock P.L. 1990: Tectonic landforms expressing strain at the Karliova continental triple junction (E. Turkey). *Annales Tectonicae* 4, 182–195.

USGS 2005: United States Geological Survey, National Earthquake Information Center. Web page: http://www.usgs.gov/

Wallace R.E. 1968: Earthquake of August 19, 1966, Varto Area, eastern Turkey. *Bulletin of the Seismological Society of America* 58, 11–45.

Wells D.L. & Coppersmith S.R. 1994: New Empirical Relationships among magnitude Rupture length, Rupture width, Rupture Area and surface Displacement. *Bulletin of Seismological Society of America* 84, 974–1002.

Yılmaz A., Terlemez İ. & Uysal Ş. 1988: Some stratigraphic and tectonic characteristics of the area around Hınıs (southeast of Erzurum). *Bulletin of the Mineral Research and Exploration* 108, 1–21.

Zabcı C., Akyüz H.S. & Sançar T. 2017: Palaeoseismic history of the eastern part of the North Anatolian Fault (Erzincan, Turkey): Implications for the seismicity of the Yedisu seismic gap. *Journal of Seismology* 21, 1407–1425. https://doi.org/10.1007/s10950-017-9673-1